Journal of Energy Storage 48 (2022) 103822

Contents lists available at ScienceDirect

Journal of Energy Storage

journal homepage: www.elsevier.com/locate/est

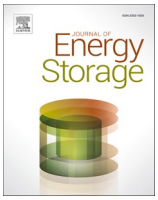

Optimal operation of energy hubs integrated with electric vehicles, load management, combined heat and power unit and renewable energy sources

Ruihua Li [a,*], Sanam SaeidNahaei [b]

[a] School of Electrical and Mechanical Engineering, Xuchang University, Xuchang, Henan 461000, China
[b] Department of Physics, Yeungnam University, Gyeongsan, South Korea

ARTICLE INFO

Keywords:
Demand-side management
Renewable resources
Uncertainty
Monte Carlo
Grasshopper search algorithm
Electric vehicle
Optimal energy scheduling

ABSTRACT

As an integral part of multi-energy systems, the energy hub acts a major task in developing the flexibility, efficiency, and reliability. Due to the increasing progress of science and human communities and the rise in air pollutants and Earth temperature, the need for renewable energies and electric vehicles has increased. The only challenge to the use of new energies is the uncertainty in their production due to the lack of continuous solar irradiation and wind in different hours of the day. Accordingly, this paper addresses an optimal load dispatch form for an energy hub to decrease the total costs of the energy hub, such as exploitation costs and CO_2 emission costs. This energy hub includes a heat storage unit, combined heat and power (CHP) unit, photovoltaic (PV) arrays, gas boiler, wind turbine (WT), and electric vehicles (EV). EV uncertainty is modeled via Monte Carlo simulation and a developed algorithm based on grasshopper search is adopted for dealing with future uncertainties in electricity price. Moreover, the proposed model considers the electric and thermal demand response (DR) methods comprehensively. Herein, three scheduling scenarios are discussed with different charge/discharge and DR settings. The numerical and graphical results demonstrate that, by choosing a coordinate charge/discharge mode for the EVs, the final costs are successfully reduced. Compared to Scenario 1, the total costs of Scenario 2 are reduced by 12%. Consequently, it can be obvious that the EVs' matched charge/discharge is successfully decreased the energy costs for the consumers. Compared to Scenario 2, the total costs of Scenario 3 are decreased by 5.76%. The results also indicate that by implementing the DR programs, total consumer costs can be further decreased.

1. Introduction

Due to the rise in environmental and economic limitations in the today's world, application of dispersed generation, which often uses renewable energies, along with electric vehicles is markedly increasing. On the large-scale, either of these technologies can have damaging effects on the electricity grid; however, with suitable consumption-side management and programming, technologies and energy storage resources can reduce these effects. Accordingly, the effect of the integrated aggregation of plug-in electric vehicles (PEVs) to the grid for the charge/discharge process and the resulting grid instability, especially at load peak time, is the main challenge to the use of these vehicles [1]. In other words, in the past, energy systems were exploited separately; today, however, due to the rise in the demand, limited amount of fossil fuels, and necessity of sustainable energy transfer, the integrated use of energy systems is a major challenge worldwide. Therefore, energy stability has become a major issue. Different aspects of the sustainable energy concept have so far been examined. In [2], the combination and integration of using and scheduling different energy structures are introduced in the form of a multi-energy grid, as a way for the maximum use of the existing energy structures. Multi-energy grids are power delivery systems that include several energy carriers including electricity, gas, regional heat, and hydrogen. In fact, integrating different energy structures means to connect them to one another and allow them convert into one another. This cooperation occurs in a unit called energy hub, where different energy carriers can be converted into one another, stored, or transferred [3]. In fact, an energy hub functions as the link between consumers, producers, and energy infrastructure. There has always been a need for storing electric energy. This need has become

Abbreviations: EV, electric vehicle; PEV, plug-in EV; PHEV, plug-in hybrid EV; EVA, EV aggregator; DG, distributed generation; ESS, energy storage system; RDER, renewable distributed energy resource.

* Corresponding author.
E-mail address: raiderlee@163.com (R. Li).

https://doi.org/10.1016/j.est.2021.103822
Received 27 August 2021; Received in revised form 12 December 2021; Accepted 13 December 2021
Available online 11 January 2022

Nomenclature

Index

T	time period
l	stochastic simulation
J	electric vehicle

Parameters

OM_{PV}	PV maintenance factor
OM_{WT}	WT maintenance factor
OM_{PV}	CHP unit maintenance factor
OM_{B}	boiler maintenance factor
OM_{HS}	heat storage unit maintenance factor
$ugri_{gri}$	electric grid's CO_2 emission factor
u_{CHP}	CHP unit's CO_2 emission factor
U_{B}	boiler unit's CO_2 emission factor
γ_t^G	natural gas cost in period t
C_{tre}	costs of the CO_2 pollutant emission treatment unit
$C_{R,J}^{EV\cdot}$	cost of changing the *j*th battery of the EV
$E_{PUT,J}^{EV}$	total discharge/charge capability of the *j*th battery
$\pi_{DR}^{E,UP}/\pi_{DR}^{E,down}$	costs of the ascending/descending setting unit of the DR electric program
$\pi_{DR}^{H,UP}/\pi_{DR}^{H,down}$	costs of the ascending/descending setting unit of the DR thermal program
$MR_{up}^{E}/MR_{down}^{E}$	maximum ratios of electricity demand transferred up/down
$MR_{up}^{H}/MR_{down}^{H}$	maximum ratios of thermal demand transferred up/down
$E_{min,j}^{EV}/E_{min,j}^{EV}$	lower/upper bound of the electric energy stored in the *j*th EV
$P_{ch,max,j}^{EV}$	maximum bound of the charge power of the *j*th EV
$P_{dch,max,j}^{EV}$	maximum bound of the discharge power of the *j*th EV
$P_{ch,max}^{EV}/P_{dch,max}^{EV}$	upper bounds of the charge/discharge power of all EVs
$\eta_{ch}^{EV}/\eta_{dch}^{EV}$	EV charge/discharge efficiency
$t_{arr,j}/t_{dep,j}$	entry/exit time of the *j*th EV
H_{min}^{S}/H_{max}^{s}	maximum /minimum bound of the stored heat of the heat storage unit
$\eta_{ch}^{s}/\eta_{dch}^{s}$	charge/discharge efficiency of the heat storage unit
$p_{ch,max}^{s}/p_{dch,max}^{s}$	maximum bounds of the charge/discharge power of the heat storage unit
p_i^{pv}	PV output power at time *t*
P_t^{WT}	WT output power at time *t*
P_t^{EL}	uncharged electric demand of the EV charge in period *t*
P_t^{HL}	thermal demand in period *t*
η_{CHP}^{e}	efficiency of CHP gas conversion to electricity
η_{CHP}^{h}	efficiency of CHP gas conversion to heat
η_B	steam boiler efficiency
G_{max}^{CHP}	maximum allowable natural gas at CHP inlet
G_{max}^{B}	maximum allowable natural gas at boiler inlet
P_{max}^{H}	maximum limit of thermal power transfer of the heat pipe
L_{buy}^{max}	maximum transfer power when purchasing electricity from the electricity grid
L_{sell}^{max}	maximum transfer power when selling electricity to the electricity grid
π_t^{buy}	lower bound of the forecast electricity price in period *t*
Δt	duration of each period
T	total number of periods in the scheduling cycle
L	total number of stochastic simulations
J	total number of EVs

Continuous variables

π_t^{buy}/π_t^{sell}	electricity purchase/sales price in period *t*
P_t^{buy}/P_t^{sell}	electricity purchase/sales power in period *t*
C_{OM}	operation and maintenance price of the energy carriers
C_{EM}	total costs of CO_2 emission treatment
C_{OM}^{RDER}	maintenance and operation costs of RDERs
C_{OM}^{CHP}	maintenance and operation costs of CHP unit
C_{OM}^{B}	maintenance and operation cost of the boiler
C_{OM}^{HS}	maintenance and operation cost of the heat storage unit
C_{BAT}	EV battery depreciation cost
C_{EDR}/C_{HDR}	DR electric/thermal program cost of the energy hub
G_T^{CHP}	natural gas consumed by the CHP at time *t*
G_t^{B}	natural gas consumed by the boiler at time *t*
$P_T^{E,UP}/P_t^{E,down}$	electric power transferred up and down by DR program at time *t*
$P_t^{H,UP}/P_t^{H,down}$	thermal power transferred up and down by DR program at time *t*
H_T^{S}	thermal energy stored in the heat storage unit at time *t*
$P_{CH,j,t}^{EV}/P_{ch,j,t}^{EV}$	charge/discharge power of the *j*th EV at time *t*
$E_{j,t}^{EV}$	electric energy stored in the *j*th EV at time *t*
$E_{j,t-1}^{EV}$	energy stored in the *j*th EV at time t-1
$P_{ch,t}^{S}/P_{dch,t}^{S}$	charge/discharge power of the heat storage unit at time *t*
P_t^{ECHP}	CHP output electric power at time *t*
P_t^{HCHP}	CHP thermal power at time *t*
P_t^{HB}	boiler thermal power at time *t*
β_t	uncertainty of the electricity price at time *t*
P_{wit}	the output of the *i*th wind generator at time *t*
ν_{in}	cut-in wind speed
ν_{out}	cut-out wind speed
ν_r	wind speed rate

Binary variables

$I_t^{E,up}$	indicator of raising the electricity demand; 1 denotes an ascending change in the electricity demand status in period t; otherwise, $I_t^{E,up} = 0$.
$I_t^{E,down}$	indicator of reducing the electricity demand; 1 denotes a descending change in the electricity demand status in period t; otherwise, $I_t^{E,down} = 0$.
$I_t^{H,up}$	indicator of raising the thermal demand; 1 denotes an ascending change in the electricity demand status in period t; otherwise, $I_t^{H,up} = 0$.
$I_t^{H,down}$	indicator of reducing the electricity demand; 1 denotes a descending change in the electricity demand status in period t; otherwise, $I_t^{H,down} = 0$.
$Z_{j,t}^{ch}$	charging mode of the *j*th EV; 1 denotes that the *j*th EV is charged in period t; otherwise, $Z_{j,t}^{ch} = 0$.
$Z_{j,t}^{dch}$	discharging status of the *j*th EV; 1 denotes that the *j*th EV is discharged in period t; otherwise, $Z_{j,t}^{dch} = 0$.
k_t^{ch}	charging status of the heat storage unit; 1 denotes that the heat storage unit is charged in period t; otherwise, $k_t^{ch} = 0$.
k_t^{dch}	discharging status of the heat storage unit; 1 denotes that the heat storage unit is discharged in period t; otherwise, $k_t^{dch} = 0$.
r	robust parameter

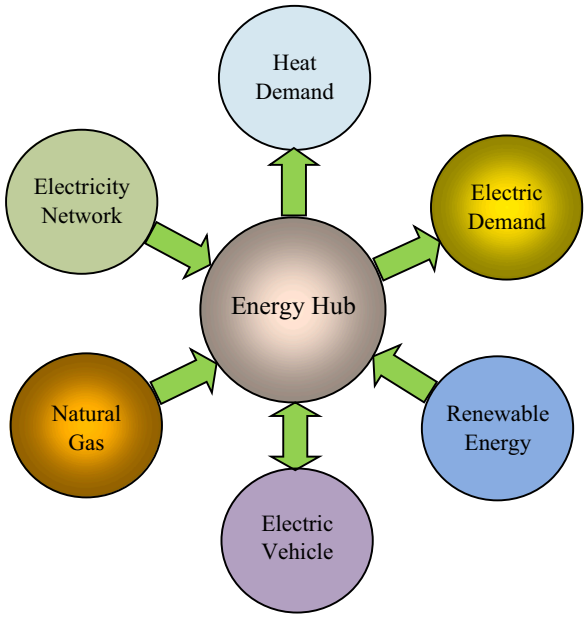

Fig. 1. General concept of the energy hub.

more pronounced due to the growth of RES in electricity production. Due to the uncertainties in RES products, the storage of the produced electricity by them and its use in emergencies have become more important. Fig. 1 illustrates the concept of integrated energy.

Currently, many energy systems such as electricity and natural gas are used separately. Nowadays, with the increase in and advancement of two- and three-energy production technologies, it is essential to establish a link between energy systems. If different energy infrastructure, such as natural gas, heating, and cooling, are properly aggregated and integrated, the energy system use will be improved for different reasons [4]. These reasons include the expanded use of small-scale energy resources to produce and heating, continuous increase in energy demand, difficulty and very costly replacement/development of energy infrastructure, global policies to reduce greenhouse gasses, further use of sustainable and bio-compatible energy sources, and promising advances in energy technologies (e.g., increasing the energy efficiency of small-scale power plants with two and three energy products) [5]. Several studies have been conducted on multi-energy systems' load dispatch. In [6], a combined energy division framework was proposed for multiple microgrids in an energy system integrated with the heat of electricity power, in which various factors, e.g., production cost, commerce costs, thermal discomfort cost, load characteristic, etc., were considered. By considering economic dispatch constraints, reduction of air transfer lines, and self-repair mechanisms, a decentralized and real-time system was suggested in [7]. The advanced model can be used in all electricity consumption sectors (residential, commercial, industrial), installation companies, and electricity grid. In [8], there was a trade-off between maximizing the renewable penetration level to the energy hub and minimizing the associated costs. In this paper, a novel optimal scheduling model was recommended that allowed variable renewable penetration level (PRL) which can be regulated into energy hub (EH) to be used for minimizing the operational costs of the system. As determined by the grid operator, RPL was assumed as a setting for the scheduling model. The micro-energy system was the developer of the micro-system, a major energy use carrier in the future; the use of energy price as a controllable source helped improve the micro-energy system (MES) optimization potential [9]. In the first stage, based on the Euclidean ball method, a general method was proposed for modeling the MES steady-state energy balance equation. Then, based on the effect of replacing multiple energies in the backdrop of connecting multiple energies, the concept of price-based integrated demand response was presented. In [10], household energy management based on the smart residential energy hub (SREH) with the inputs of electricity and natural gas was designed for modern households. The models of energy use and control strategies were presented, respectively, via the physical characteristics and preferences of the household users. A multi-objective optimization problem for energy resource allocation in SREH was presented and the scheduling program was offered for the equipment by using energy along with classified conventional devices. In [11], a combined renewable system comprising WT, PV cell, diesel, and battery was proposed. A new method was presented for determining the optimal size of the units in the combined systems based on the degree of coordination between electricity production and consumption intervals, such that the minimum economic costs were incurred. The electricity adaptation rate was introduced as a criterion for determining the optimal number of units in the proposed combined system. This technique was developed based on the multi-objective PSO algorithm. In [12], a multi-objective optimization approach based on stochastic simulation was introduced for measuring combined systems based on renewable energy. This method integrated an optimization module based on multi-objective genetic algorithm; an uncertainty module that used the Latin Hypercube method and Monte Carlo simulation to generate uncertainty scenarios, and a simulation module for simulating the power system in real operational conditions. In [13], an integrated method was presented for designing electric hubs as a combination of optimization, multi-criterion evaluation, and decision-making. The cost of energy, investment cost, CO_2 emission, grid integration level, use of RE, system flexibility, loss of load probability were the criteria used for evaluating the plan. In [14], a multi-objective programming model was presented for multi-energy systems based on operational financial system and energy effectiveness. Moreover, two types of cooling and heating storage energy hubs were designed. In [15], an integrated programming model was proposed to examine the technical and economical performance of an independent microgrid based on RE. In [6], a mixed-integer non-linear programming method was presented for smart DGs and the thermal energy managing of buildings and supporting water demand in a microgrid. In [17], a novel multi-objective method presented to solve an economic and emission power dispatch. Various papers have been presented on this topic in recent years; in [18], attempts were made to present a detailed explanation on the integration of RE in CHP systems. In [19], an optimal planning form was proposed for a multi-energy hub system. In [20], an electrical and thermal energy managing was created for a conventional residential energy hub to reduce the energy cost while taking into account customer settings. This work was examined only by connecting one EV to the system, and the large-scale EV installation was not modeled in the energy hub. In [21], a method based on reliable search area was used to solve the pollution and power dynamic distribution problem. In this method, in addition to developing the proposed algorithm based on the general search, the effect of the energy storage system in the power dynamic optimal problem was studied. In [22], a biogeography-based optimization method by solving the power dynamic problem was used while considering EVs.

According to the literature review section, different factors should be considered in the planning and operation of multiple energy systems as:

- In each converter and technology of storage in energy hub, the related size is important;
- In energy hub systems, the type of conversion and storage technologies are important;
- The technology of control methodology for power flow is important as well.

The mentioned specifications govern the overall operational effectiveness, and also determine the reliability of the system once subjected to an increasing demand. Based on a review of the literature, it is concluded that the connection of EVs to the grid has posed new

challenges to power system management.

The recent published systems lack some specifications as: The possibility of combining a large fleet of distributed energy sources (DER) and adapting to increasing energy demand in the future so that increasingly strict environmental laws are observed [1]. Inefficiency of these systems in managing power distribution based on user consumption on a regional scale [8]. Also, problems with energy efficiency are emerging, as multiple generation energy systems and decentralized generation technologies have received more attention. Therefore, more flexible energy substrates are required in terms of operation and distribution [8–10].

Having suitable methods for improving grid management is an important issue when there are numerous RES. Therefore, a weakness of previous methods is being trapped in local points and the absence of a powerful general searcher in these algorithms. Meanwhile, the adaptation of the probability distribution with uncertain data is tiresome. Also, the obtained results of optimization may not meet the limitations of states that are not included. Considering the world warm concerns, the carbon emission calculation and management is converted into an important investigate topic. The existing methods used for carbon cycle calculation and analysis include the statistical method, lifecycle analysis method, and grid-based model. In general, few papers on optimal load dispatch from the energy hub have considered EV extensive access, which is not suitable for analyzing the effect of increasing EV penetration in the energy hub load. Meanwhile, the majority of the existing DR program based on load dispatch models have considered only electric DR. To more energy consumption reduction, both DR thermal and electrical methods must be considered. In addition, the majority of the studies have not considered a robust and reliable optimization method to deal with electricity price uncertainty. To overcome these deficiencies, a powerful optimization model for energy hub load dispatch is proposed in the present study. Accordingly, the most important contributions and highlights of this paper include:

1 An energy hub model is developed while considering environmental factors, in which both thermal and electrical DR methods are taken into account for further reduction of the user's energy construction cost.
2 A developed optimization approach based on the grasshopper search algorithm is presented to consider the uncertainty of the electricity price.
3 The suggested energy hub form considers large-scale EV random access and EV battery depreciation cost to realize EV charge/discharge economic management.

2. Energy hub model

2.1. Energy hub conception

Energy carriers, including electricity and heat, along with other solid, liquid, and gas fuels, form the middle link in the energy supply chain among primary resources and the final consumer. An energy system comprising more than one carrier is referred to as the multi-carrier energy system or an energy hub. In this structure, transductors play a major role in the energy system due to the dependence of one carrier on another. Due to the importance of electricity and its increasingly critical role as a middle carrier with excellent features, energy studies are mainly focused on power system studies [23]. Moreover, gas fuel is of special importance in studies due to easy access, inexpensiveness, and existence of sufficient sources. Increasing attention to environmental issues and creating new protocols such as the Kyoto Protocol have increased this importance; this type of energy is now preferred to heavy fuels such as mazut and coal. The network structure of the gas energy carrier, its geographical expanse, and introduction of novel WT have contributed to the considerable attention paid to the dependence of gas and electricity grids compared to other forms of

Fig. 2. Input-output port model for the energy hub.

infrastructure. The presence of transductors made energy grids (that used to be separate, and produced, transferred, and consumed energy at multiple levels with a relatively similar structure) dependent on one another in many respects. Therefore, research on the effects of different energy carriers on one another in this new dependent setting has received considerable attention [24]. The input/output port model or the energy hub is displayed in Fig. 2 and formulated by:

$$\begin{bmatrix} F_1 \\ F_2 \\ \vdots \\ F_n \end{bmatrix} = \begin{bmatrix} C_{11} & C_{12} & \cdots & C_{1m} \\ C_{21} & C_{22} & \cdots & C_{2m} \\ \vdots & \vdots & \ddots & \vdots \\ C_{n1} & C_{n2} & \cdots & C_{nm} \end{bmatrix} \begin{bmatrix} I_1 \\ I_2 \\ \vdots \\ I_n \end{bmatrix} \tag{1}$$

where m-vector I denotes input energy carriers, n-vector F denotes output energy flows, C indicates the coupling matrix, and each element of matrix C represents the energy efficiency.

2.2. Energy hub modeling

Here, the energy hub is considered with energy production, utilization, and storage systems. Fig. 3 illustrates the brief illustration of the employed energy hub arrangement. RDERs in the energy hub include PV array and WT. Electricity demand includes the basic electricity load and EV charge load that can be supplied by the electricity grid, CHP, and RDERs. The hub's excessive electricity can be sold to the electricity grid. The energy hub system produces thermal energy through CHP and boiler to meet the heat demand. As demonstrated in Fig. 3, the natural gas input can be separated into two main components which are consumed by the CHP and boiler, respectively. υ denotes the dispatch feature ($0 \le \upsilon \le 1$) which shows the distribution of natural gas utilization among the boiler and CHP.

3. Optimization representation

3.1. EV charge form

3.1.1. EV driving distance

The daily EV driving distance can be represented as a logarithmic distribution function [25], i.e., $S \sim Log-N(\mu_s, \sigma_s^2)$:

$$f_s(x) = \frac{1}{\sqrt{2\pi}\sigma_s x} \exp\left(-\frac{(\ln x - \mu_s)^2}{2\sigma_s^2} \right) \tag{2}$$

where $\mu_s = 3.2$ and $\sigma_s = 0.88$. Fig. 4 illustrates the daily EV driving distance based on the probability distribution [1].

3.1.2. EVs' entry and exit time

EV owners stop charging in the morning when they leave the house. The exit time of an EV follows normal distribution [26], i.e., $t \sim N(\mu_{dep}, \sigma_{dep}^2)$:

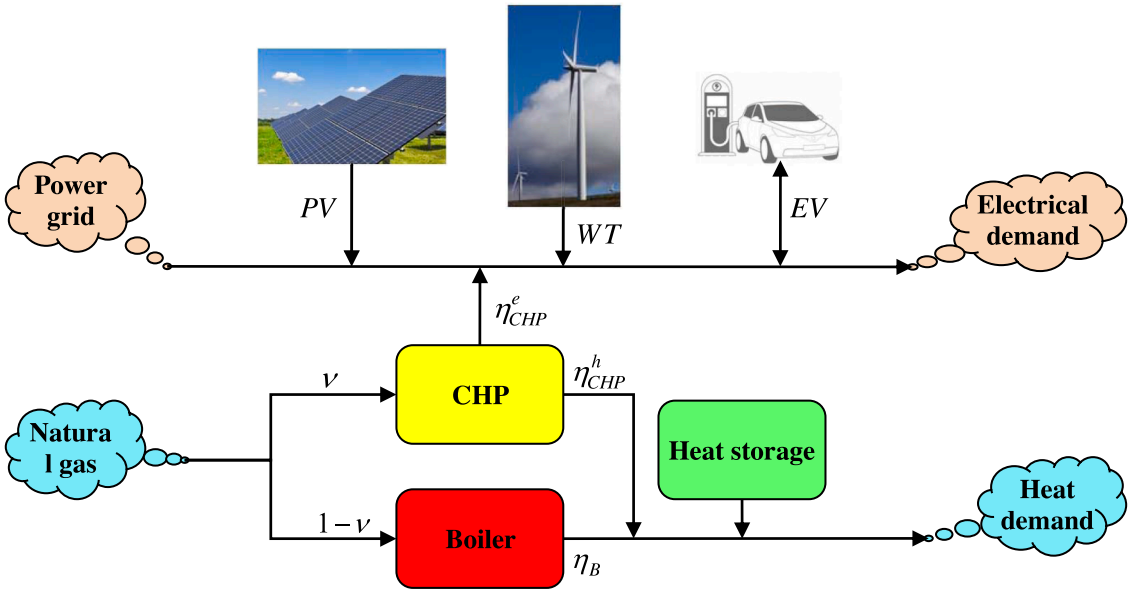

Fig. 3. A review of the proposed energy hub.

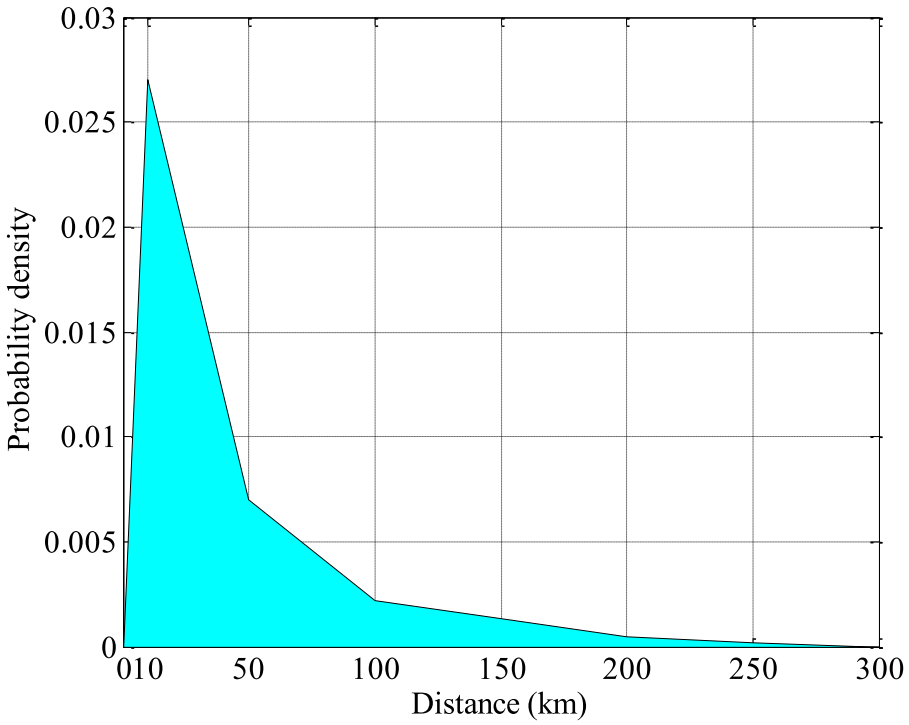

Fig. 4. The daily EV driving distance with probability distribution function.

$$f_{dep}(t)=\begin{cases}\frac{1}{\sqrt{2\pi}\sigma_{dep}}\exp\left(-\frac{(t-\mu_{dep})^2}{2\sigma^2_{dep}}\right) & 0<t\le\mu_{dep}+12\\ \frac{1}{\sqrt{2\pi}\sigma_{dep}}exp\left(-\frac{(1-24-\mu_{dep})^2}{2\sigma^2_{dep}}\right) & \mu_{dep}+12<t\le 24\end{cases} \quad (3)$$

where μ_{dep}= 3.24 and σ_{dep}= 8.92. The EV owners typically start charging in the evening when they arrive at home. The arrival time of the EV is formulated by normal distribution function, i.e., $t \sim N(\mu_{arr}, \sigma^2_{arr})$:

$$f_{arr}(t)=\begin{cases}\frac{1}{\sqrt{2\pi}\sigma_{arr}}exp\left(-\frac{(t+24-\mu_{arr})^2}{2\sigma^2_{arr}}\right) & 0<t\le\mu_{arr}-12\\ \frac{1}{\sqrt{2\pi}\sigma_{arr}}exp\left(-\frac{(t-\mu_{arr})^2}{2\sigma^2_{arr}}\right) & \mu_{arr}-12<t\le 24\end{cases} \quad (4)$$

where μ_{arr}= 17.6 and σ_{dep}= 3.4. The probability distributions of the exit and entry times of these EVs are shown in Fig. 5.

3.1.3. EV's uncoordinated charge

The daily driving distance and the EV's charge time are autonomous of each other. Therefore, the load characteristic of each EV's charge is

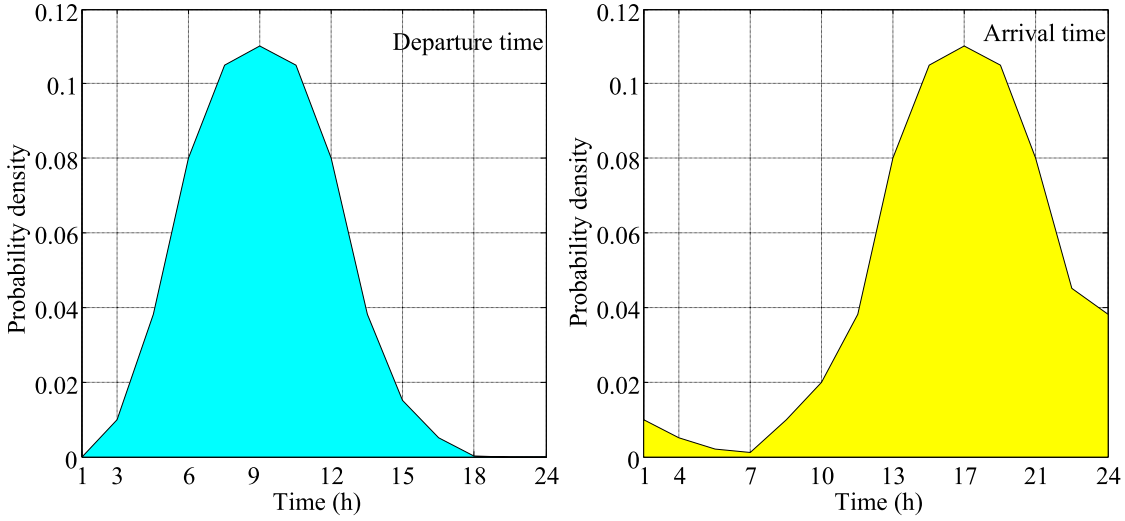

Fig. 5. Probability distributions of the EVs' exit and entry times.

obtained by random tests for simulating the driving distance and the charge onset time of each EV. Herein, the Monte Carlo technique is adopted to simulate each EV's charge load characteristics. Then, by placing each EV's load characteristics, we can obtain the overall charge load characteristics. To achieve the logical charge load characteristics, *L* simulations are performed for J EVs. The specific stages are as follows:

Stage 1: Start the iteration l= 1,
Stage 2: Start the EV j= 1,
Stage 3: Based on the entry time probability density function, generate a random number from the charge onset time of the jth EV.
Stage 4: Based on the driving distance probability density function, generate a random number from the driving distance of the jth EV.
Stage 5: Calculate the electricity demand for charging and charge times of the jth EV.
Stage 6: Adapt the charge load characteristics of the jth EV.
Stage 7: If $j < J$, increase the jth indicator of EV by one unit and return to Stage 3; otherwise, proceed to the next stage.
Stage 8: If $l < L$, increase the lth indicator of iteration by one unit and return to Stage 2; otherwise, generate the output of the results and the process ends.

3.2. The objective function

The objective function of the suggested model for minimizing the overall costs includes implementation costs when comparing the energy hub with the electricity grid, operation and maintenance costs of energy carriers, CO_2 emission treatment costs, EV batteries' depreciation costs, and implementation cost resulting from DR electric/thermal programs:

$$\min\left\{\sum_{t}\left(\pi_{t}^{buy}.P_{t}^{buy}-\pi_{t}^{sell}.P_{t}^{sell}\right).\Delta t+C_{OM}+C_{BAT}+C_{EM}+C_{EDR}+C_{HDR}\right\} \tag{5}$$

The energy hub system integrates RDERs, CHP units, boiler, and thermal storage system. Therefore, the maintenance and operation cost of this system is explained by:

$$C_{OM=}\ C_{OM}^{RDER}+C_{OM}^{CHP}+C_{OM}^{B}+C_{OM}^{HS} \tag{6}$$

The operation and maintenance cost of energy carriers comprises fuel costs and maintenance costs. The operations and maintenance costs of RDERs are formulated by [27]:

$$C_{OM}^{RDER}=\sum_{T}\left(P_{T}^{PV}.OM_{PV}+P_{T}^{WT}.OM_{WT}\right).\Delta t \tag{7}$$

The operation and maintenance costs of CHP unit comprise fuel cost and maintenance cost, one gets:

$$C_{OM}^{CHP}=\sum_{t}\left(G_{t}^{CHP}.\gamma_{t}^{G}+\left(P_{t}^{ECHP}+P_{t}^{HCHP}\right).OM_{CHP}.\Delta t\right) \tag{8}$$

The operation and maintenance costs of the boiler consist of fuel and maintenance costs:

$$C_{OM}^{B}=\sum_{t}\left(G_{t}^{B}.\gamma_{t}^{G}+P_{t}^{HB}.OM_{B}.\Delta t\right) \tag{9}$$

The maintenance cost of the heat storage system is considered by multiplying the total charge-discharge thermal cost by a maintenance cost factor:

$$C_{OM=}^{HS}\sum_{t}\left(P_{dch,t}^{S}+P_{ch,t}^{S}\right).OM_{HS.\Delta t} \tag{10}$$

To realize the EV charge/discharge economic management, the EV batteries' depreciation cost is considered and defined as follows:

$$C_{BAT}=\sum_{t}\sum_{J}\left(P_{ch,j,t}^{EV}+P_{dch,j,t}^{EV}\right).\Delta t\frac{C_{R,J}^{EV}}{E_{PUTJ}^{EV}} \tag{11}$$

By taking into account the CO_2 emission cost in the proposed problem, this model can be defined as:

$$C_{EM}=\sum_{t}C_{M}.\left(P_{t}^{BUY}.U_{grid}+\left(P_{t}^{ECHP}+P_{t}^{HCHP}\right).U_{CHP}+P_{t}^{HB}.U_{B}\right).\Delta t \tag{12}$$

Using DR programs can modify peak load and fill the valley load by promising the consumers about a reduction in load demand in a period with a high price and a rise in load demand in a period with a low price. However, after the customers change their main electricity consumption pattern, it causes discomfort, and this discomfort level affects consumers' tendency to participate in DR methods. Therefore, the cost of implementing DR electric/thermal programs (i.e., consumers' discomfort cost resulting from load variation) should be accounted for. Herein, it is assumed that increasing/decreasing the load demand in each scheduling period causes discomfort for the consumer; the discomfort cost has a positive relationship with the degree of load change [28], expressed as:

$$C_{EDR}=\sum_{t}\left(\pi_{DR}^{E,down}.P_{t}^{p,down}+\pi_{t}^{E,down}.P_{t}^{E,up}\right).\Delta T \tag{13}$$

$$C_{HDR}=\sum\left(\pi_{DR}^{H,DOWN}.P_{t}^{H,down}+\pi_{DR}^{H,up}.P_{t}^{H,up}\right).\Delta T \tag{14}$$

3.3. Operational constraints of the system

3.3.1. DR electric program constraints

The DR electric program constraints are considered as:

$$\sum_t P_t^{E,up} = \sum_t P_t^{E,down} \tag{15}$$

$$0 \le P_t^{E,up} \le MR_{UP}^{E}.P_t^{EL}.I_t^{E,down} \tag{16}$$

$$0 \le P_t^{E,down} \le MR_{down}^{E}.P_t^{EL}.I_t^{E,down} \tag{17}$$

$$0 \le I_t^{E,up} + I_t^{E,down} \le 1 \tag{18}$$

The energy hub should consider the sum electricity utilization constant in the planning cycle, which is constrained by Eq. (15). The upper bounds of the electric charge transferred up and down are constrained by Eqs. (16) and (17), respectively. Eq. (18) ensures that the energy hub cannot simultaneously transfer electric charge up and down.

3.3.2. DR thermal program constraints

The DR thermal program constraints are considered as:

$$\sum_t P_t^{H,up} = \sum_t P_t^{H,down} \tag{19}$$

$$0 \le P_t^{H,up} \le MR_{up}^{H}.P_t^{HL}.I_t^{H,up} \tag{20}$$

$$0 \le P_t^{H,down} \le MR_{down}^{H}.P_t^{HL}.I_t^{H,down} \tag{21}$$

$$0 \le I_t^{H,up} + I_t^{H,down} \le 1 \tag{22}$$

Similar to the DR electric program, Eq. (19) models the balance between the thermal loads transferred up and down. The upper bounds of the thermal load transferred up and down are constrained by Eqs. (20) and (21), respectively. Eq. (22) prevents the energy hub from transferring the thermal load up and down simultaneously.

3.3.3. EV constraints

EV constraints are given below:

$$E_{j,t}^{EV} = E_{j,t-1}^{EV} + P_{ch,j,t}^{EV}.\Delta t.\eta_{ch}^{EV} - \frac{P_{dch,j,t}^{EV}.\Delta t}{\eta_{dch}^{EV}} \tag{23}$$

$$E_{min,j}^{EV} \le E_{j,t}^{EV} \le E_{max,j}^{EV} \tag{24}$$

$$0 \le P_{dch,j,t}^{EV} \le P_{dch,max,j}^{EV}.Z_{j,t}^{dch} \tag{25}$$

$$0 \le P_{dch,j,t}^{EV} \le P_{dch,max,j}^{EV}.Z_{j,t}^{dch} \tag{26}$$

$$Z_{j,t}^{ch} + Z_{j,t}^{dch} = 1, \forall j,\ t \in \left[t_{arr,j}, t_{dep,j}\right] \tag{27}$$

$$Z_{j,t}^{ch} + Z_{j,t}^{dch} = 0, \forall j,\ t \notin \left[t_{arr,j}, t_{dep,j}\right] \tag{28}$$

$$0 \le \sum_j P_{ch,j,t}^{EV} \le P_{ch,max}^{EV} \tag{29}$$

$$0 \le \sum_j P_{ch,j,t}^{EV} \le P_{ch,max}^{EV} \tag{30}$$

The batteries' energy equilibrium limitation is known in Eq. (23). To protect the EVs' batteries, the stored energy system must be restricted to a confident range, as reflected in Eq. (24). The maximum charge and discharge power of the EVs is constrained in electronic equations. The maximum value of charge and discharge power of the EVs is constrained in Eqs. (25) and (26). When the EVs are connected to the energy hub, they cannot be simultaneously charged and discharged, which is constrained by Eq. (27). When the EVs are not connected to the energy hub, they are neither charged nor discharged, which is constrained by Eq. (28). In this study, when the EVs are charged, the maximum transfer power among EVs and the energy hub is constrained by Eq. (29). Similarly, in discharged mode, the maximum transfer power is constrained by Eq. (30).

3.3.4. Constraints of the heat storage system

$$H_t^S = H_{t-1}^S + P_{ch,t}^S.\Delta t.\eta_{Ch}^S - \frac{P_{dch,t}^S.\Delta t}{\eta_{dch}^S} \tag{31}$$

$$H_{min}^S \le H_t^S \le H_{max}^S \tag{32}$$

$$0 \le P_{ch,t}^S \le P_{ch,max}^S.K_t^{ch} \tag{33}$$

$$0 \le P_{dch,t}^S \le P_{dch,max}^S.K_t^{dch} \tag{34}$$

$$k_t^{Ch} + k_t^{dch} \le 1 \tag{35}$$

The heat storage unit's thermal energy balance constraint is given in Eq. (31). Like EV batteries, the thermal energy stored in the heat storage system must be restricted in a confident range expressed by Eq. (32). The maximum charge and discharge power of the heat storage unit is constrained in Eqs. (33) and (34), respectively. Eq. (35) ensures that the heat storage unit cannot be simultaneously charged and discharged.

3.3.5. Energy balance of the energy hub system

$$P_t^{buy} + P_t^{PV} + P_t^{WT} + P_t^{ECHP} + \sum_t P_{dch,j,t}^{EV} + P_t^{E,down} = p_t^{EL} + \sum_t P_{ch,j,t}^{EV} + P_t^{sell} + P_t^{E,up} \tag{36}$$

$$P_t^{HCHP} + P_t^{HB} + P_t^{S} + P_t^{H,down} = P_t^{HL} + P_{ch,t}^{S} + P_t^{H,up} \tag{37}$$

$$p_t^{HB} = G_t^{B}.LHV.\eta_{CHP}^{e}/\Delta T \tag{38}$$

$$P_t^{HCHP} = G_t^{CHP}.LHV.\eta_{CHP}^{H}/\Delta t \tag{39}$$

The energy hub model should maintain the equilibrium among electrical energy generating unit and demand, which is limited by Eq. (36). In the meantime, the thermal energy generating unit must meet the demand for heating, which is limited by Eq. (37). Eq. (38) denotes the thermal generation of the boiler unit based on the amount of input natural gas. Based on the amount of input natural gas and CHP yield, electricity and heat generation of the CHP is calculated by Eq. (39), respectively.

3.3.6. Natural gas input constraint

The CHP and boiler should have the minimum and maximum constraints of the natural gas input. Constraints are expressed below:

$$0 \le G_t^{CHP} \le G_{max}^{CHP} \tag{40}$$

$$0 \le G_t^{B} \le G_{max}^{B} \tag{41}$$

The heat pipe should have minimum and maximum constraints of the thermal power transfer, which can be as follows:

3.3.7. Thermal power transfer constraints

$$0 \le P_T^{HCHP} + P_t^{HB} + P_{dch,t}^S - P_{ch,t}^S \le P_{max}^H \tag{42}$$

3.3.8. Transfer power constraints

The transfer of energy among the grid and the energy hub to ensure the safety of operation of the power system cannot exceed the transfer limit.

$$0 \le P_t^{buy} \le L_{buy}^{max} \tag{43}$$

$$0 \le P_t^{sell} \le P_{sell}^{max} \tag{44}$$

When purchasing electricity energy from the electricity grid, the maximum transfer power is constrained by Eq. (43); when selling the electricity power to the electricity grid, it is limited with Eq. (44).

3.3.9. Wind power model

Energy produced by the wind system is in accordance with the relevant wind speed. Therefore, its model is as follows:

$$P_{wt}^{t} = \begin{cases} P_{wt,r}, v_r < v^t < v_{cout} \\ P_{wt,r}\dfrac{v^t - v_{cin}}{v_r - v_{cin}}, v_{cin} < v^t < v_{cout} \\ 0, otherwise \end{cases} \tag{45}$$

while, P_{wt}^{t} defines the wind turbine production power at hour t, $P_{wt,r}$ is the nominal wind turbine power in KW. v^t, v_r, v_{cin}, v_{cout} are the wind speed at t hour nominal speed, low cut-off speed and high cut-off speed in m/s, respectively.

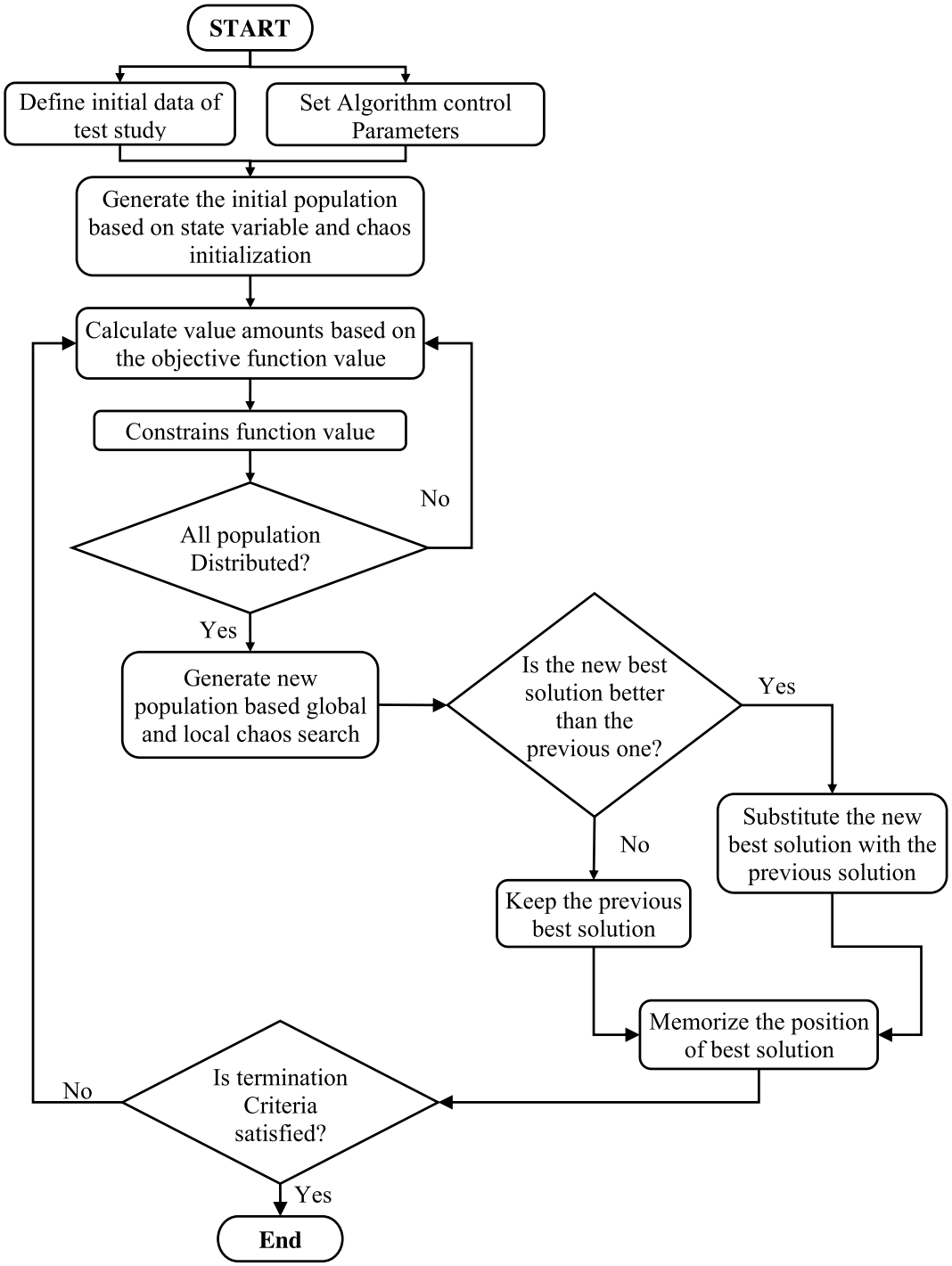

Fig. 6. The proposed algorithm's flowchart for solving the problem.

3.4. Uncertainty modeling

To deal with electricity price uncertainty, the set of uncertainties is as follows:

$$\pi_t^{buy} \in \left[\pi_t^{buy}, \pi_t^{buy} + d_t\right] \tag{46}$$

where π_t^{buy} is the real-time price of electricity in period t, which varies at a limited price, and means that X is different. $[\pi_t^{buy}, \pi_t^{buy} + d_t].\pi_t^{buy}$ indicates the lower limit of the electricity price predicted in period t. d_t indicates the maximum price uncertainty (financial risks) in period t, and a higher value d_t means higher price uncertainty. When $d_t = 0$, this indicates that the price of period t is already known. So, it can be modeled the degree of price uncertainty by introducing the parameter and variable β_t, which is as follows:

$$\pi_t^{buy} \in \left[\pi_t^{buy}, \pi_t^{buy} + \beta_t d_t\right] \tag{47}$$

$$0 \le \beta_t \le 1 \tag{48}$$

$$\sum_t \beta_t \le r \tag{49}$$

Where the variable β_t indicates the degree of price uncertainty in period t. $\beta_t = 0$ indicates a situation where there is no price uncertainty in period t, while $\beta_t = 1$ indicates a situation where there is maximum price uncertainty in period t. The parameter limits the maximum value to the sum of r. Therefore, the resistance level of the solution can be controlled by the β_t parameter due to the uncertainty of the electricity price. The maximum value of r is the value of the total periods in the timeline horizon, and the higher the value of r, the higher the resistance level of the answers. The objective can then be transformed as follows:

$$in\left\{\sum_t \begin{array}{c}\left(\pi_t^{buy}.p_t^{buy}.\pi_t^{sell}.P_t^{sell}\right).\Delta t + C_{OM} + C_{BAT} + C_{EM} + C_{HDR} + \\ max\left\{\sum_t P_t^{buy}.\Delta t.\beta_t.d_t\right\}\end{array}\right\} \tag{50}$$

The proposed optimization problem and constraints equations are an optimization problem that is solved with the proposed algorithm in the next section.

4. Developed grasshopper optimization algorithm

GOA is an evolutionary computation method that is inspired by the behavior of grasshoppers when looking for food. Since the goal of this article is to present a developed model, the standard model of this algorithm is generally presented. Refer to [29] for more information. Mathematical equations for GOA are created by using a specified food source for searching the grasshoppers' tendencies. Then, the attack behavior of grasshoppers is affected by their social interaction, the gravity force, and wind transfer. By using the following equation, the grasshopper's position in the space can be obtained:

$$X_i = S_i + G_i + W_i \tag{51}$$

Here, X_i is the position of grasshopper i^{th} in the space; S_i is the advantage of social interaction obtained by grasshopper i^{th}; S_i, G_i, and W_i are the mutual social, gravitational, and air transfer effects of the grasshopper, respectively.

$$S_i = \sum_{j=1, j\neq i}^{NGH} s\left(\left|X_j - X_i\right|\right)\frac{\left(X_j - X_i\right)}{D_{ij}} \tag{52}$$

$$S(u) = fe^{-u/lg} - e^{-u} \tag{53}$$

The description of the performance of the social force among grasshoppers is calculated by Eq. (53). U is the distance between grasshoppers, f is the intensity of gravity, and lg is the distance of the gravity.

Table 1
Parameters of the EVs used [25].

Numerical value	Type
1000	Maximum capacity (kWh)
600	Initial storage (kWh)
100/1000	Lower/upper limit of stored heat energy (kWh)
150	Maximum charging power (kW)
150	Maximum discharging power (kW)
0.9	Charging efficiency

Here, for optimization, the values of 0.5 for f and 1.5 for lg are assumed. Since the effect of gravitational force on grasshopper swarm behavior is insignificant, it is neglected and the effect of wind is modeled as the best global solution. Finally, using the following, the grasshopper's position can be updated.

$$X_i^k = C\left[\sum_{j=1, j\neq i}^{NGH} C\frac{\left(X_{max}^k - X_{min}^k\right)}{2} S\left(\left|X_j^k - X_i^k\right|\right)\frac{\left(X_j^k - X_i^k\right)}{D_{ij}^k}\right] + X_{gbest}^k \tag{54}$$

$$C = C_{max} - iter\frac{C_{max} - C_{min}}{iter_{max}} \tag{55}$$

A novel idea in solving complex problems with non-linear functions is to use the chaotic search method in smart methods in order to enhance the capabilities of the smart algorithm. The chaotic technique formulated by non-linear and non-convex functions that receive more attention now. The proposed chaotic method for solving the problem can be expressed as:

$$\begin{aligned}\frac{dx}{dt} &= \sigma(y - x)\\ \frac{dy}{dt} &= x(\rho - z) - y\\ \frac{dz}{dt} &= xy - \beta z\end{aligned} \tag{56}$$

where x, y, z, belong to the state of the system in time. Moreover, σ, $\rho$and β show the system parameters. This model inspired of ordinary differential programs that was first considered by Edward Lorenz. It is considerable for having irregular solutions for special parameter values and initial conditions. Specifically, the Lorenz attractor is a set of irregular solutions of the Lorenz system [30]. This emphasizes that physical systems can be totally deterministic; still, they are not inherently predictable even in the absence of quantum effects. The form of the Lorenz attractor itself, when graphically plotted, may look like a butterfly. Accordingly, the chaotic theory can be defined by the following steps:

Step 1: The chaos and algorithm control values are set.
Step 2: The initial population generated among the variable lower and upper bounds.
Step 3: The decision variables map.
Step 4: Chaotic variables convert with decision variables.
Step 5: Evaluate the new solution by decision variables.

Fig. 6 shows how the proposed optimization algorithm relates to the problem.

5. Case study

5.1. Information of test system and settings

This subsection sets the scheduling horizon at one day and, after that, divides the total time horizon into 24 periods by setting 1 h as the calculation period. It is assumed that 300 EVs exist in this energy hub. For effective modeling and scheduling the EVs, the EV batteries'

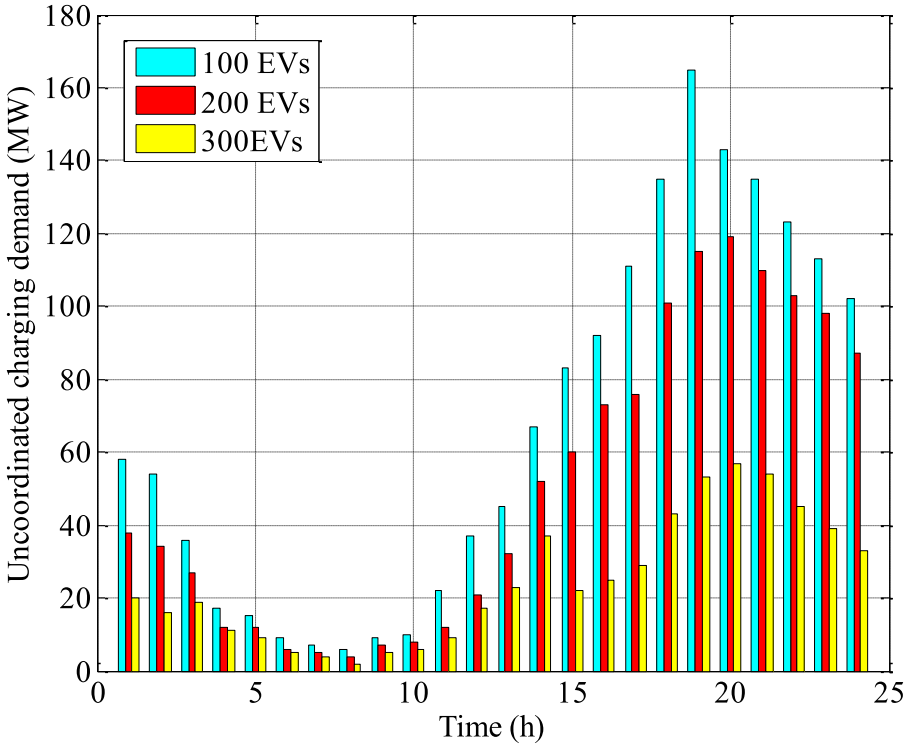

Fig. 7. EV uncoordinated charge.

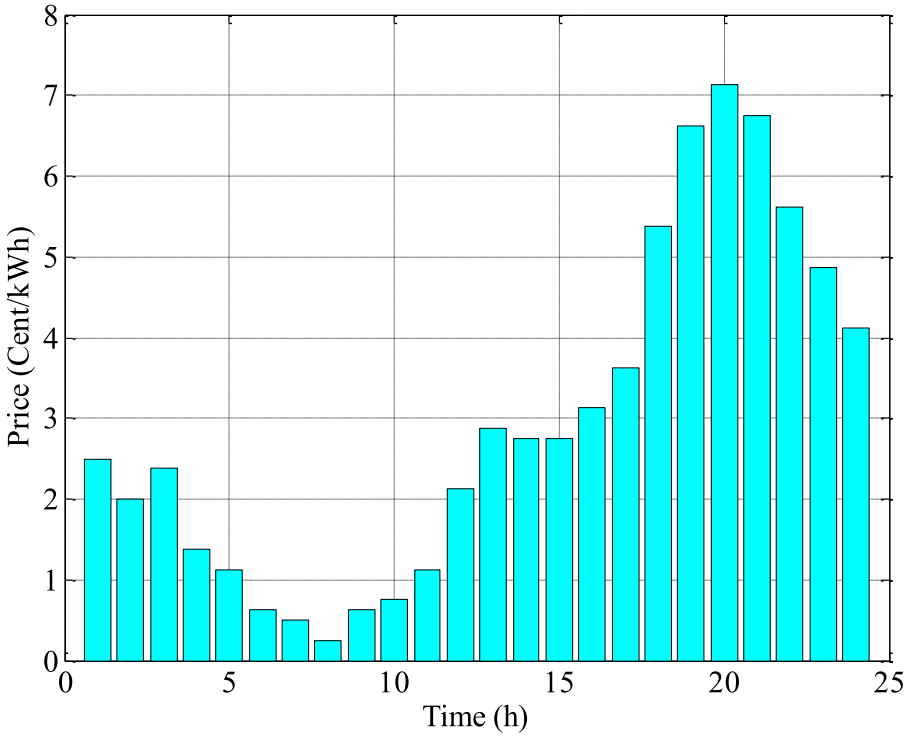

Fig. 8. Lower bound of the forecast electricity price.

characteristics are taken into account. The EV charge energy equals the daily energy consumption. The essential variables of the EVs are listed in Table 1 [25]. According to the Monte Carlo technique, the uncoordinated charge demand of all EVs can be obtained. Fig. 7 displays the uncoordinated charge load with various numbers of EVs. Electricity prices in real time differ from the price limits. The lower bound of the forecast electricity prices is given in Fig. 8. Maximum price uncertainties (d_t) are assumed to be 20% of the lower bound of the forecast price. Maximum price uncertainties (d_t) can be obtained based on the existing forecast methods. In realistic model, the numeric value of 20% can be changed based on the forecast real results. It is assumed that the extra electricity sales price to the gird is 10% lower than the lower limit of the

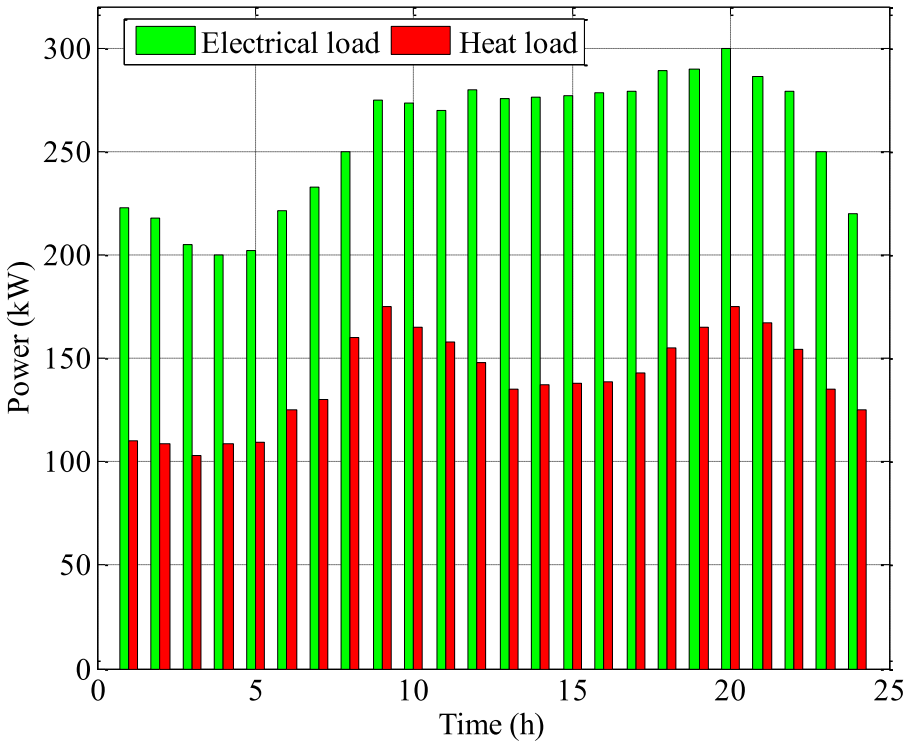

Fig. 9. Electric and thermal load demand.

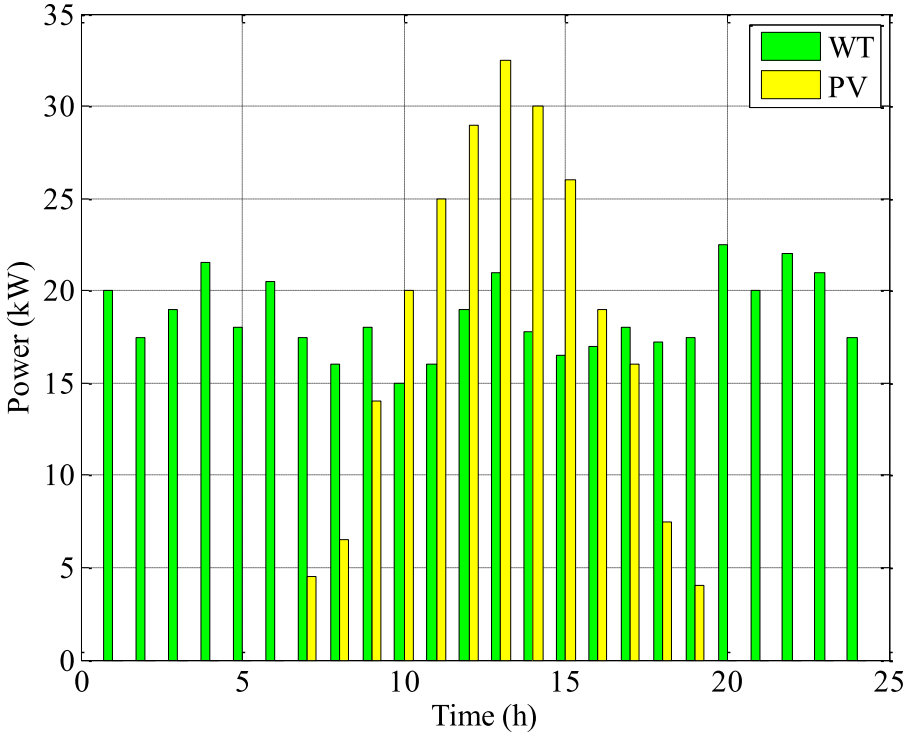

Fig. 10. PV and WT output power profiles.

electricity prices. The initial demand (without EV charge loads) and the thermal load demand are given in Fig. 9. The PV and WT output power characteristics are presented in Fig. 10. The employed parameters of the heat storage system are listed in Table 2. The other useful data are tabulated in Table 3 [31].

5.2. Discussion and analysis of the results

In this section, three planning scenarios are taken into account to evaluate the effect of EV's coordinated charge/discharge mode and DR methods on the planning results. The uncertainties of price will be taken into account in all these scenarios. Three types of planning scenarios can

Table 2
Parameters of the heat storage unit.

Type	Numerical values
Maximum capacity (kWh)	1000
Initial storage (kWh)	600
Lower/upper limit of stored heat energy (kWh)	100/1000
Maximum charging power (kW)	150
Maximum discharging power (kW)	150
Charging efficiency	0.9
Discharging efficiency	0.9

Table 3
Other parameters used in the simulation.

Parameter	Unit	Amount	Parameter	Unit	Amounts
OM_{PV}	cent/kWh	0	${MR_{up}}^{E}$	–	0.50
OM_{WT}	cent/kWh	0	${MR_{down}}^{E}$	–	0.20
$OMCHP$	cent/kWh	2.0	MR_{up}^{H}	–	0.50
OM_{B}	cent/kWh	2.7	${MR_{down}}^{H}$	–	0.20
OM_{HS}	cent/kWh	0.5	λ_t^G	cent/m^3	22
u_{grid}	kg/kWh	0.187	C_{tre}	cent/kg	3.36
u_{CHP}	kg/kWh	0.177	LHV	kWh/m^3	9.7
u_B	kg/kWh	0.177	η_{CHP}^{e}	–	0.35
$\pi_{DR}^{E.up}$	cent/kWh	0.10	η_{CHP}^{h}	–	0.45
$\pi_{DR}^{E.down}$	cent/kWh	0.10	η_B	–	0.8
$\pi_{DR}^{H.up}$	cent/kWh	0.10	$G_{\max}^{CHP}$	m^3/h	100
$\pi_{DR}^{H.down}$	cent/kWh	0.10	$G_{\max}^{B}$	m^3/h	100

be described as follows:

Scenario 1: To establish the usefulness of the EVs' coordinated charge/discharge mode in decreasing the total costs, a basic case planning scenario is taken into account, e.g. EVs approve the uncoordinated charge mode.
Scenario 2: Compared to Scenario 1, the EVs in this scenario choose the coordinate charge/discharge mode.
Scenario 3: Here, to confirm the effectiveness of EV programs, DRs choose the coordinate charge/discharge mode. DR methods are also considered.

5.2.1. Economic dispatch analysis

The results of dispatching electric and thermal energy under Scenario 1 are given in Fig. 11. It is evident from Fig. 11a that the EV's charge loads are concentrated under the uncoordinated charge mode during the night. This is because EV owners usually start charging when they arrive home in the evening. CHP in the high electricity price periods generates electricity (h 9–20), which reduces the system's electricity utilization cost. As the CHP produces electricity and thermal power simultaneously, it is clear from Fig. 11b that it also produces thermal energy in peak-price times and the boiler produces thermal energy in low-price times (h 5–10 and h 20–24), thereby reducing the system's thermal energy consumption cost. Based on Fig. 11b, the heat storage unit participates in the load scheduling under Scenario 1; the extra thermal energy produced by CHP is used to charge the heat storage system in 15–18 h As denoted by the negative values in Fig. 11b, the heat storage unit is discharged in 2–4 h

The results of dispatching electric and thermal energy under Scenario 2 are given in Fig. 12. We can see that with the coordinated charge/discharge, EV charge loads are transferred from the high to low electricity price periods. This is because a change in the EVs' charge load reduces the system's electricity consumption cost. As shown in Fig. 12a, the EVs are not discharged in each period. This is because of the cost of depreciating electrical units is high, and electricity discharged by electric vehicles must be redeemed, which is done by electric vehicle owners to meet driving needs. In addition, the behavior of selling electricity to the grid or supplying electricity to meet load demand increases the cost of battery depreciation for owners of electric vehicles.

The obtained results of dispatching electric and thermal energy in Scenario 3 are given in Fig. 13. Compared to scenarios 1 and 2, after running the DR electric and thermal plans, the electric and thermal load demand is varied. Fig. 13 illustrates the level of loading without and with implementing electric and thermal DR programs.

It is observed from the DR electric and thermal programs that the electricity demand of the energy hub in high electricity price times (9–21 h) is transferred to a low electricity price time to reduce the costs of purchasing electricity from the grid. In high electricity price periods, the energy hub increases the CHP output, such that it can reduce the electricity purchase cost. Since the CHP produces electric and thermal energy simultaneously, it increases the output of thermal energy to increase the output of the electric energy in high electricity price periods. In this way, after using the DR program, to consume the increased output of thermal energy, the total thermal demand is increased in the high electricity price period (13–19 h). The comparison of the costs of different scenarios is presented in Table 4. Compared to Scenario 1, the total costs of Scenario 2 are reduced by 12%. Consequently, it can be obvious that the EVs' matched charge/discharge can successfully decrease the energy costs for the consumers. Compared to Scenario 2, the total costs of Scenario 3 are decreased by 5.76%. This indicates that

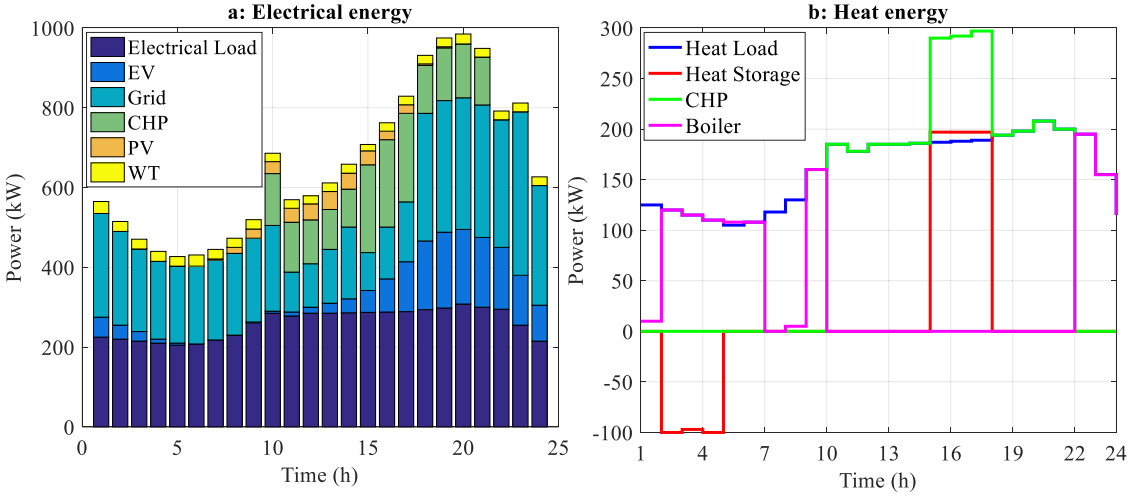

Fig. 11. Optimal dispatch results in the Scenario 1.

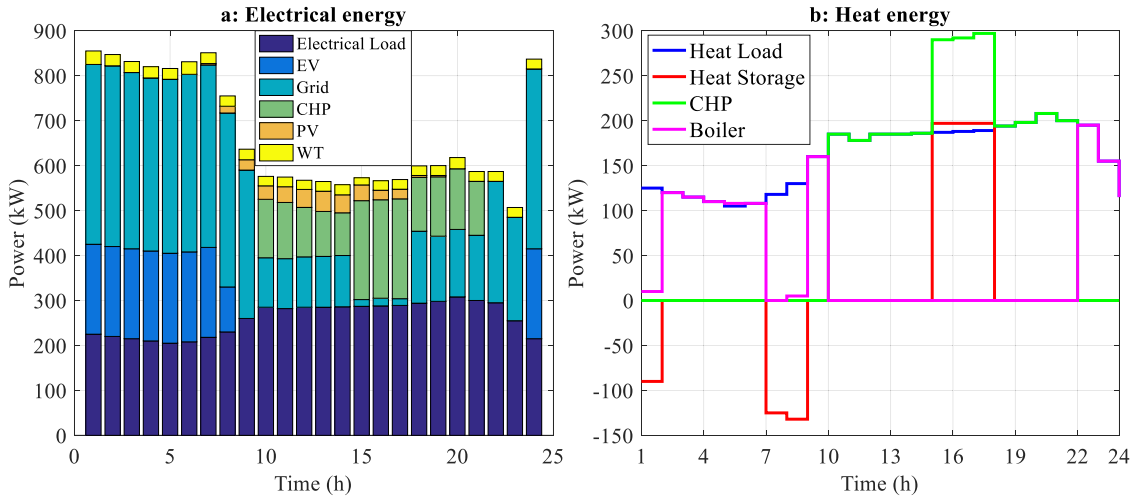

Fig. 12. Optimal dispatch results in the Scenario 2.

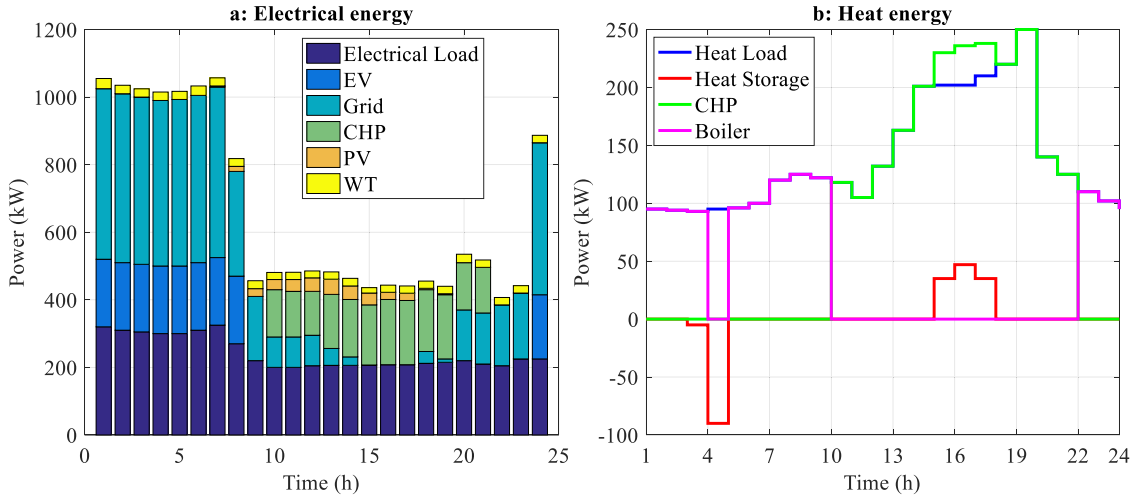

Fig. 13. Optimal dispatch results in the Scenario 3.

Table 4
Comparing the costs of different scenarios.

	Scenario 1	Scenario 2	Scenario 3
Total cost ($/day)	632.251	590.323	556.341
CPU time (min)	< 1 min	< 1 min	< 1 min

DR programs can more decrease consumers' total costs by means of displacing the loads.

5.2.2. *Effect of EV depreciation cost*

Based on the high costs of EV depreciation, EV owners do not wish to allow EV discharge to prolong EV battery life. Therefore, EV depreciation cost has a significant effect on planning results. This sub-section deals with the effects of EV depreciation costs. The general costs in all scenarios with and without taking into account EV reduction costs are presented in Fig. 14. It is observed that the total costs under the scenario without considering EV depression are markedly reduced compared to the scenario considering EV depreciation; this denotes that the EV reduction cost cannot be ignored by the users.

Based on the planning results of all scenarios, Scenarios 2 and 3 (i.e., EVs using coordinated charge/discharge mode) are used as an example. The optimal dispatch results in Scenario 2 without taking into account EV reduction costs are presented in Fig. 15. It is clear from Fig. 15a that the EVs are charged in low electricity price times, which is similar to the results of Scenario 2 taking into account EV reduction cost. However, it is evident that the EVs are discharged in the high electricity price period (13–20 h), so that the amount of purchased electricity is reduced when the price is high, as denoted by negative values in Fig. 15. The optimal dispatch results in Scenario 3 without allowing for EV reduction costs are presented in Fig. 16. In similar way with Scenario 2, the EVs are charged in low electricity price times (1–10 h and 22–24 h) and discharged in high electricity price times (12–20 h), which is able to decrease the electricity price when the price is high. We can also observe that the energy hub sells the extra electrical energy to the electricity grid to gain profit in a high electricity price period (18 h). It can be seen that when the reduction cost is not considered, EVs are repeatedly charged and discharged more to decrease the total costs of the energy system.

5.3. *Impact of strong parameter on uncertainty*

Electricity price uncertainty can be modeled with a powerful parameter. Therefore, the planning results are influenced by the choice of a powerful parameter. It is necessary to discuss the effect of a powerful parameter on the results. The total costs in different robust parameter values under the three programming scenarios are shown in Fig. 17. It can be seen that with increasing power r under all three

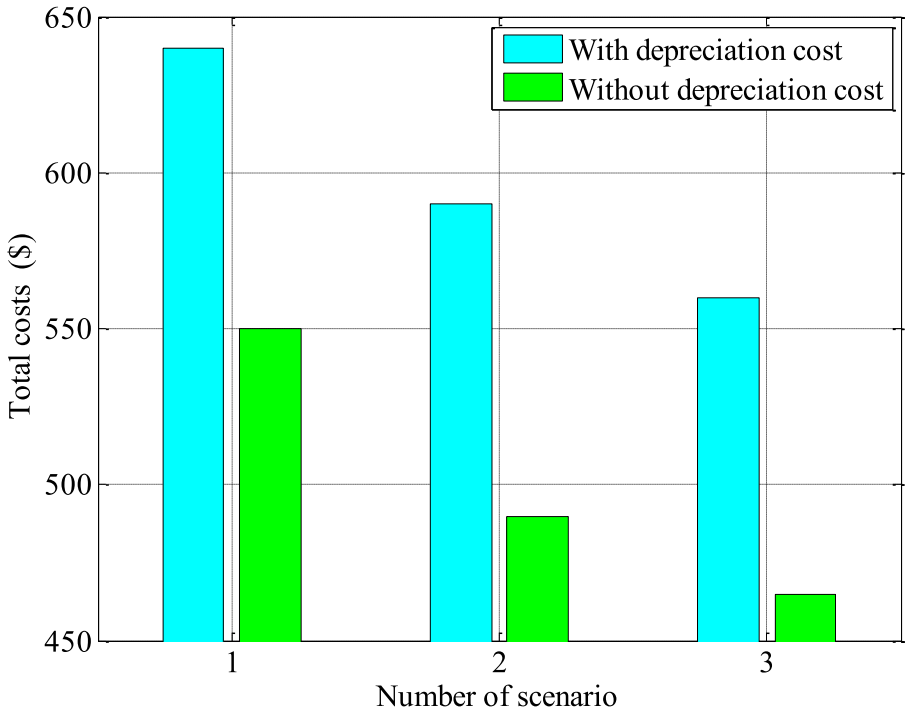

Fig. 14. Total costs in all scenarios with and without taking into account EV reduction cost.

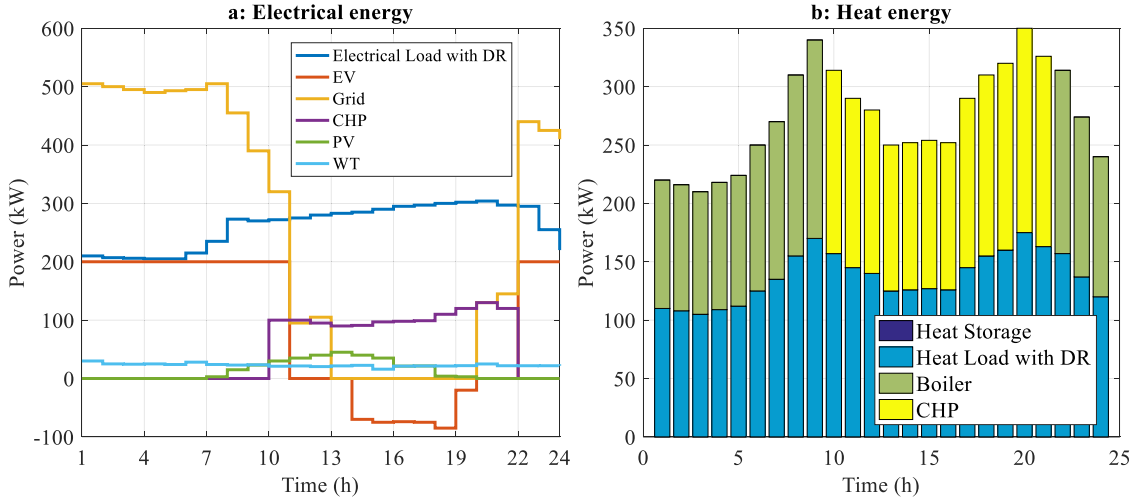

Fig. 15. Scheduling results in Scenario 2 lacking EV reduction cost.

dimensions, the overall costs increase. The reason for this is that larger values indicate greater uncertainty in electricity prices, which will pose a greater financial risk to the system. When $r = 0$, the powerful optimization model becomes the deterministic model, so the energy center system has the lowest price. Thus, it provides a powerful trading parameter between optimization and solution strength. In the load management process, the operator needs to select a suitable powerful parameter according to the level of real uncertainty of electricity prices.

5.4. Proposed algorithm's performance analysis

In this section, the performance of the proposed algorithm is compared with other genetic optimization and particle clustering algorithms for the problem proposed in this paper. To make a fair comparison for all three algorithms, the number of iterations to be 100 and the number of initial populations to be 50 are considered. Other control parameters are used based on the best performance of these algorithms in other research and various test functions to consider each with maximum search capability. The convergence results of the three algorithms are shown in Fig. 18.

As can be seen from the figure, the proposed algorithm performed much better than the other two algorithms and also had less standard deviation. The proposed algorithm was able to achieve its optimal answer from approximately 30 iterations.

6. Conclusion

Optimal load dispatch is a major engineering optimization problem for supporting the capable operation of hub energy models. In this study, a new model for energy managing with the developed GOA for an energy hub is proposed. This energy hub included a CHP unit, gas boiler, heat storage system, PV arrays, WT, and EV. EV uncertainty was modeled via

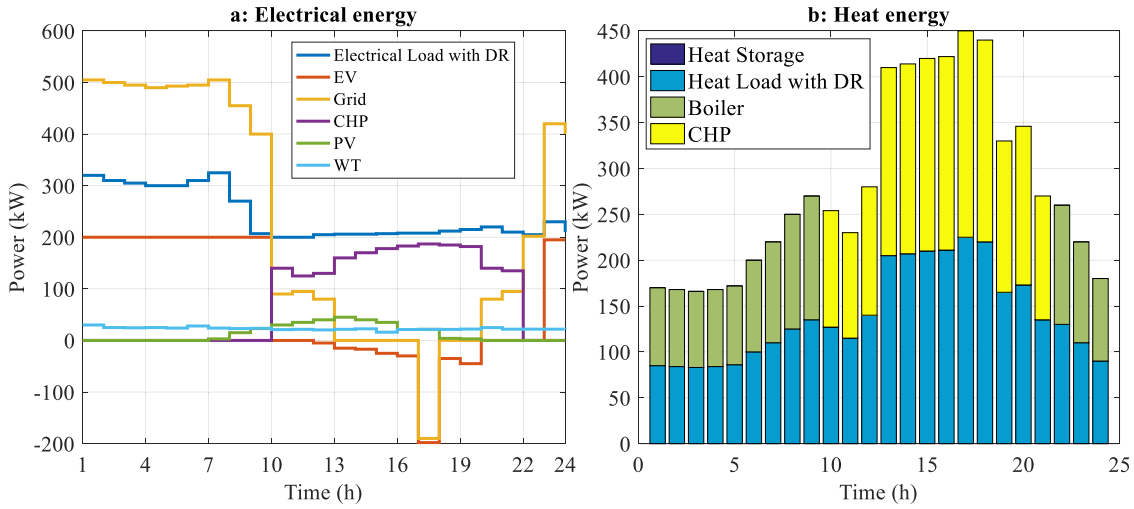

Fig. 16. Scheduling results in Scenario 3 lacking EV reduction cost.

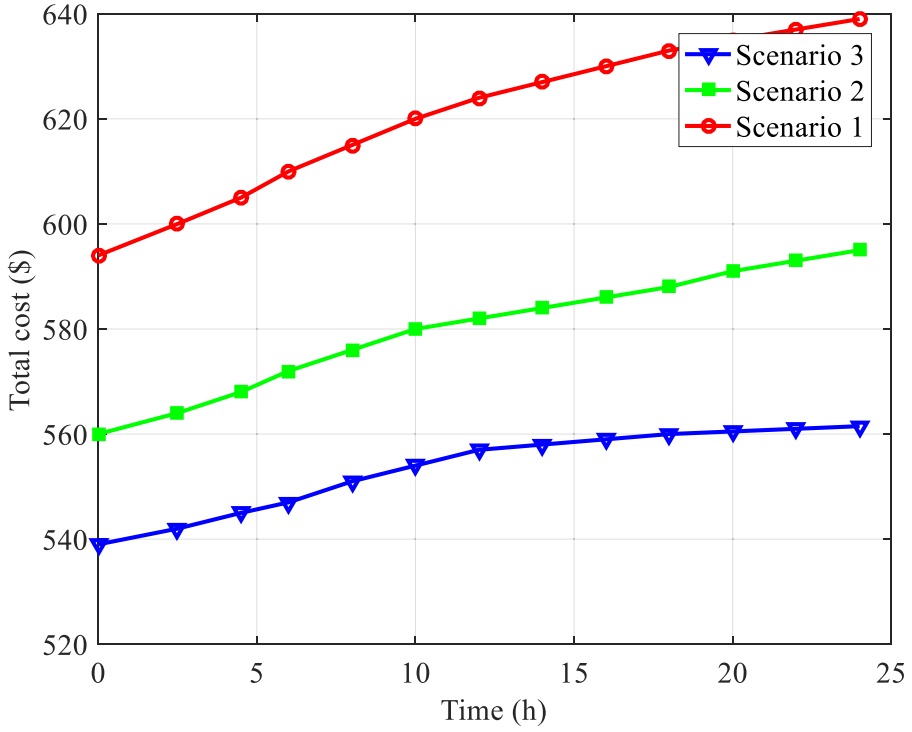

Fig. 17. General costs by considering the electricity price uncertainty.

Monte Carlo simulation and the developed algorithm based on grasshopper search was adopted for dealing with the future uncertainties in electricity price. To evaluate the performance of the studied system, three scheduling scenarios were discussed, including EV uncoordinated charge, and EV coordinated charge/discharge with and without DR methods. The numerical results shown that the EV coordinated charge/discharge mode can reduce the total costs by 12% compared to the uncoordinated charge mode. The results also showed that by implementing the DR methods, the total cost can be reduced by about 5%. The findings indicated that the proposed method showed the trade-off among optimality and robustness of the solutions based on the real uncertainty level of electricity price. Discussions were also made about the effect of EV depreciation. It was shown that when the depreciation cost was ignored, the EV would play a major role in the load management of the energy hub. This paper provided new insight into the load transfer of the energy hub with the extensive deployment of EVs. Also, if the prices of electricity are uncertain in the relevant uncertainty sets, according to the proposed robust optimization approach, the cost of the whole energy system is always less than the obtained cost. In addition, compared to the other algorithms i.e., GA and PSO methods, the suggested algorithm can converge with appropriate accuracy and find the global optimal. This ability can be achieved in less than 40 iterations, which is very convenient compared to other algorithms.

CRediT authorship contribution statement

Ruihua Li: Resources, Software, Supervision, Writing – review & editing, Investigation, Conceptualization. **Sanam SaeidNahaei:** Project administration, Writing – review & editing, Data curation, Formal analysis, Methodology, Validation.

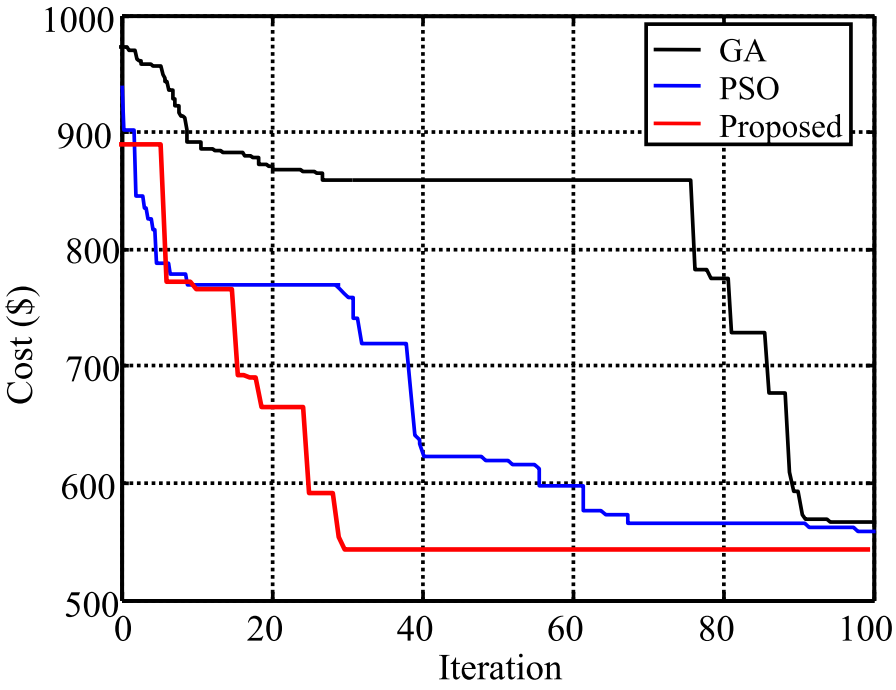

Fig. 18. Comparing the convergence of different algorithms.

Declaration of Competing Interest

The authors declare that they have no known competing financial interests or personal relationships that could have appeared to influence the work reported in this paper.

Acknowledgment

This research was financially supported by Henan Province Science and Technology Project (182102210508).

References

[1] X. Lu, Z. Liu, L. Ma, L. Wang, K. Zhou, N. Feng, A robust optimization approach for optimal load dispatch of community energy hub, Appl. Energy 259 (2020), 114195.
[2] Min Duan, et al., A novel hybrid prediction model for aggregated loads of buildings by considering the electric vehicles, Sustain. Cities Soc. 41 (2018) 205–219.
[3] O. Abedinia, M. Lu, M. Bagheri, An improved multicriteria optimization method for solving the electric vehicles planning issue in smart grids via green energy sources, IEEE Access 8 (2019) 3465–3481.
[4] C. Wang, et al., Modeling and analysis of a microgrid considering the uncertainty in renewable energy resources, energy storage systems and demand management in electrical retail market, J. Energy Storage 33 (2021), 102111.
[5] S. Huang, O. Abedinia, Investigation in economic analysis of microgrids based on renewable energy uncertainty and demand response in the electricity market, Energy 225 (2021), 120247.
[6] N. Liu, J. Wang, L. Wang, Hybrid energy sharing for multiple microgrids in an integrated heat–electricity energy system, IEEE Trans. Sustain. Energy 10 (3) (2018) 1139–1151.
[7] S. Rahim, N. Javaid, R.D. Khan, N. Nawaz, M. Iqbal, A convex optimization based decentralized real-time energy management model with the optimal integration of microgrid in smart grid, J. Clean. Prod. 236 (2019), 117688.
[8] H. Khani, A. Sawas, H.E. Farag, An estimation–based optimal scheduling model for settable renewable penetration level in energy hubs, Electr. Power Syst. Res. 196 (2021), 107230.
[9] Z. Chen, Y. Zhang, W. Tang, X. Lin, Q. Li, Generic modeling and optimal day-ahead dispatch of micro-energy system considering the price-based integrated demand response, Energy 176 (2019) 171–183.
[10] Q. Lu, S. Lü, Y. Leng, Z. Zhang, Optimal household energy management based on smart residential energy hub considering uncertain behaviors, Energy 195 (2020), 117052.
[11] B. Mukhopadhyay, D. Das, Multi-objective dynamic and static reconfiguration with optimized allocation of PV-DG and battery energy storage system, Renew. Sustain. Energy Rev. 124 (2020), 109777.
[12] J.J. Roberts, A.M. Cassula, J.L. Silveira, E. da Costa Bortoni, A.Z. Mendiburu, Robust multi-objective optimization of a renewable based hybrid power system, Appl. Energy 223 (2018) 52–68.
[13] A.T.D. Perera, V.M. Nik, D. Mauree, J.L. Scartezzini, An integrated approach to design site specific distributed electrical hubs combining optimization, multi-criterion assessment and decision making, Energy 134 (2017) 103–120.
[14] Y. Jia, Z. Mi, W. Zhang, L. Liu, Optimal operation of multi-energy systems in distributed energy network considering energy storage, 2017, in: Proceedings of the IEEE Conference on Energy Internet and Energy System Integration (EI2), IEEE, 2017, pp. 1–6.
[15] M.K. Kiptoo, M.E. Lotfy, O.B. Adewuyi, A. Conteh, A.M. Howlader, T. Senjyu, Integrated approach for optimal techno-economic planning for high renewable energy-based isolated microgrid considering cost of energy storage and demand response strategies, Energy Convers. Manag. 215 (2020), 112917.
[17] V.P. Sakthivel, M. Suman, P.D. Sathya, Combined economic and emission power dispatch problems through multi-objective squirrel search algorithm, Appl. Soft Comput. 100 (2021), 106950.
[18] M.A. Bagherian, K. Mehranzamir, A comprehensive review on renewable energy integration for combined heat and power production, Energy Convers. Manag. 224 (2020), 113454.
[19] D. Huo, S. Le Blond, C. Gu, W. Wei, D. Yu, Optimal operation of interconnected energy hubs by using decomposed hybrid particle swarm and interior-point approach, Int. J. Electr. Power Energy Syst. 95 (2018) 36–46.
[20] F. Brahman, M. Honarmand, S. Jadid, Optimal electrical and thermal energy management of a residential energy hub, integrating demand response and energy storage system, Energy Build. 90 (2015) 65–75.
[21] B. El-sobky, Y. Abo-elnaga, Multi-objective economic emission load dispatch problem with trust-region strategy, Electr. Power Syst. Res. 108 (2014) 254–259.
[22] H. Ma, Z. Yang, P. You, M. Fei, Multi-objective biogeography-based optimization for dynamic economic emission load dispatch considering plug-in electric vehicles charging, Energy 135 (2017) 101–111.
[23] V. Halmschlager, R. Hofmann, Assessing the potential of combined production and energy management in industrial energy hubs–analysis of a chipboard production plant, Energy 226 (2021), 120415.
[24] H. Yang, P. You, C. Shang, Distributed planning of electricity and natural gas networks and energy hubs, Appl. Energy 282 (2021), 116090.
[25] X. Lu, K. Zhou, S. Yang, H. Liu, Multi-objective optimal load dispatch of microgrid with stochastic access of electric vehicles, J. Clean. Prod. 195 (2018) 187–199.
[26] M. Mohiti, H. Monsef, H. Lesani, A decentralized robust model for coordinated operation of smart distribution network and electric vehicle aggregators, Int. J. Electr. Power Energy Syst. 104 (2019) 853–867.
[27] Y. Duan, X. He, Y. Zhao, Distributed algorithm based on consensus control strategy for dynamic economic dispatch problem, Int. J. Electr. Power Energy Syst. 129 (2021), 106833.
[28] P. Li, Z. Wang, J. Wang, W. Yang, T. Guo, Y. Yin, Two-stage optimal operation of integrated energy system considering multiple uncertainties and integrated demand response, Energy 225 (2021), 120256.

[29] P.H. Dinh, A novel approach based on Grasshopper optimization algorithm for medical image fusion, Expert Syst. Appl. 171 (2021), 114576.
[30] Barros, Diego, Christian Bonatti, and Maria Jose Pacifico. "Up, down, two-sided Lorenz attractor, collisions, merging and switching." *arXiv preprint arXiv: 2101.07391* (2021).
[31] A. Maroufmashat, et al., Modeling and optimization of a network of energy hubs to improve economic and emission considerations, Energy 93 (2015) 2546–2558.